

Document downloaded from:

<http://hdl.handle.net/10251/157574>

This paper must be cited as:

Luján, JM.; Climent, H.; Ruiz-Rosales, S.; Moratal, A. (2019). Influence of ambient temperature on diesel engine raw pollutants and fuel consumption in different driving cycles. *International Journal of Engine Research*. 20(8-9):877-888.
<https://doi.org/10.1177/1468087418792353>



The final publication is available at

<https://doi.org/10.1177/1468087418792353>

Copyright SAGE Publications

Additional Information

This is the author's version of a work that was accepted for publication in *International Journal of Engine Research*. Changes resulting from the publishing process, such as peer review, editing, corrections, structural formatting, and other quality control mechanisms may not be reflected in this document. Changes may have been made to this work since it was submitted for publication. A definitive version was subsequently published as <https://doi.org/10.1177/1468087418792353>

Influence of ambient temperature on diesel engine raw pollutants and fuel consumption in different driving cycles.

José Manuel Luján, Héctor Climent, Santiago Ruiz, Ausias Moratal*

CMT Motores Térmicos, Universitat Politècnica de València, Spain

*Corresponding author: aumomar1@mot.upv.es. Telephone: (+34) 963877659. Postal address: CMT Motores Térmicos. Universitat Politècnica de València. Camino de Vera s/n. 46022. Valencia. Spain.

Abstract

The effect of low ambient temperature on diesel raw (Pre-DOC) pollutant emissions is analysed in two different driving cycles: NEDC and WLTC. The study is focused on hydrocarbons, carbon monoxide, nitrogen oxides and fuel consumption. Tests are conducted at cold start in a HSDI light-duty diesel engine with two levels of ambient temperature: 20 °C and -7 °C. Results showed a general detriment of pollutant emissions and brake thermal efficiency at low ambient temperatures. NO_x is increased around 250% in both cycles when running at low temperatures. Effect on HC is more noticeable in the NEDC, where it rises in 270%, compared with the 150% of increase in the WLTC. In the case of CO, uncorrelated tendencies are observed between both driving cycles. Concerning the NEDC, CO emissions increase up to 125% while at the WLTC are reduced in a 20%. Finally, from the point of view of the thermal efficiency, a reduction nearly the 10% in the NEDC is observed. However, no fuel penalty is spotted regarding the WLTC.

Keywords

Diesel engine; Pollutant emissions; Fuel consumption; Cold conditions; Driving cycles;

1. Introduction

Pollutant emissions in automotive diesel engines have become a major subject of research. Hydrocarbons (HC), carbon monoxide (CO), nitrogen oxides (NO_x) and particles are the main pollutants emitted in combustion diesel engines [1], [2] and [3]. Increasingly stringent emissions regulations are constantly motivating the automotive industry to develop new systems and strategies. As automotive cycles are being more restrictive, it is expected that the operation conditions of the test drive will consider the effect of running at lower ambient temperature. Currently, the U.S Environmental Protection Agency includes a cold cycle of FTP-75 carried out at -7 °C [4]. On the other hand, European regulation enforces, only in petrol engines, a cold start low temperature emissions test [5]. Regarding the current state of the law, it is expected that future regulations will consider low temperature emissions as regular testing.

Under low ambient temperatures, fuel consumption and pollutant emissions during the engine warm-up are critical [6]. According to the literature [7] and [8], unburned hydrocarbons and carbon monoxide are mainly emitted when engine temperatures remain low. In addition, as temperature reduces, combustion instabilities come up and eventually misfiring events may occur [9].

Tauzia et al. [10] performed a set of steady state tests at different engine loads varying the coolant and oil temperature. The authors spotted a general tendency with lowering temperature: friction losses, volumetric efficiency and ignition delay increase and NO_x reduce. Many researchers have study the effect on pollutant emissions and engine performance in cold driving cycles. In a project initiated by the Swedish Environmental Protection Agency (SEPA), Ludykar et al. [11] reported a notable increase in the tailpipe emissions of CO, HC and NO_x in a gasoline engine running in European Urban Driving tests at -7 °C and -20 °C. Weilenmann et al. [12] carried out an extensive study of low ambient temperature (-7 and -20 °C) tailpipe emissions in a fleet of gasoline (Euro 0 and Euro 3) and Diesel engines (Euro 2). Several tests were performed such as ECE, FTP-

75, IUFC15 and IRC15. Pollutants were sampled according to the bag technique, so instantaneous data were not available. CO and HC results showed that, in general terms, cold start extra emissions were lower for diesel than for gasoline vehicles. On the other hand, a relevant trend was spotted in cold start diesel NO_x emissions for lower temperatures. The authors couldn't find an explanation of this trend as the EGR system was not considered in the analysis. Dardiotis et al. [13] performed a similar study in a fleet of gasoline and diesel engines running in a NEDC at 20 and -7 °C. CO and HC showed the same tendency spotted by Weilenmann [8], being higher the effect of ambient temperature in gasoline than in diesel engines. Regarding NO_x, the authors identified the EGR rate reduction as the main cause of pollutants increase in diesel engines running at low temperatures. In case of gasoline engines, a clear tendency couldn't be found.

Most of low temperature emissions bibliography is focused in NEDC testing. But world current legislation is turning towards a more realistic emission driving analysis which includes new procedures such the WLTC and real driving engine emissions. Some authors have analysed the effect of replacing the NEDC by the new WLTC. Pavlovic et al. [14] and Tsokolis et al. [15] have spotted the increase on CO₂ in different vehicles fleet when moving from NEDC to WLTC. Giakoumis et al. [16] presented the experimental validation of an empirical emissions and engine efficiency model where NEDC and WLTC performance were compared. Diesel raw pollutants emissions were measured in a non-controlled ambient temperature test bench showing an increase of 55% NO_x and 10.8% in soot in the WLTC. Myung et al. [17] carried out a broad study of NO_x emissions in LNT equipped diesel engines comparing different driving cycles. Tests were performed between 23 and 25 °C of ambient temperature. In comparison to the NEDC the rest of driving cycles experienced a NO_x tailpipe emission increase of 90%, 50% and 550% for the WLTC, FTP-75 and US06, respectively. Marotta et al. [18] carried out an extensive study in a 21 gasoline and diesel vehicles fleet by comparing cycle average emissions between NEDC and WLTC. Tests were performed between 22-25 °C

ambient temperature. Regarding diesel engines, the authors spotted two different trends comparing WLTC to NEDC. NO_x emissions increased, while CO and HC reduced.

Lujan et al. [19] analysed the effect of low ambient temperatures on DOC efficiency in WLTC at -7 and 20 °C. Results denoted a higher negative impact on CO than on HC oxidation. Ko et al. [20] analysed the performance of a Diesel Lean NO_x Trap (LNT) measuring the NO_x concentration at both inlet and outlet. NEDC and WLTC tests were performed at 23, 14 and -5 °C ambient temperatures. Tailpipe NO_x emissions increased up to 11 and 13 times for the NEDC and WLTC respectively when running at -5°C. In addition to the NO_x analysis the authors remarked the general trend of CO and HC increase as ambient temperature gets lower.

Despite the broad bibliography on driving cycles and pollutant emissions at low temperatures, researchers have been focused either in NEDC at low temperature or in WLTC and NEDC comparison at nearly 20 °C ambient temperature. Moreover, most of emissions findings are focused on post-DOC measurements [21]. However, the presence of an aftertreatment system disturbs the analysis of the low ambient temperature effect on combustion performance as the oxidation catalyst efficiency depends on several exhaust parameters such as the exhaust gas temperature, pollutant and oxygen concentration dwell time and light of temperature lag [22].

This work addresses the lack of current bibliography by analysing the direct effect of low temperatures in both NEDC and WLTC by means of the raw emissions and fuel consumption. Emissions were sampled at the DOC upstream to identify the cause of pollutants formation in combustion processes fired at low surrounding temperatures. All emissions were sampled on line, allowing the study of pollutants along the driving cycle.

The content is structured as follows. Section 2 is devoted to the experimental setup and driving cycles description. Section 3 contains the results and analysis of the ambient temperature effect on the raw emissions and efficiency. Finally, the main conclusions are presented in section 4.

2. Experimental setup and methodology

2.1. Description of test cell and setup.

Experiments with an inline 4 cylinder, 1.6 l, turbocharged HSDI diesel engine were conducted. In Fig. 1 the engine layout is depicted, where both the High Pressure (HP) and Low Pressure (LP) Exhaust Gas Recirculation (EGR) loops are shown. An intercooler is placed between the compressor and the HP EGR inlet. The aftertreatment system, which includes a DOC and a DPF, is placed downstream the turbine.

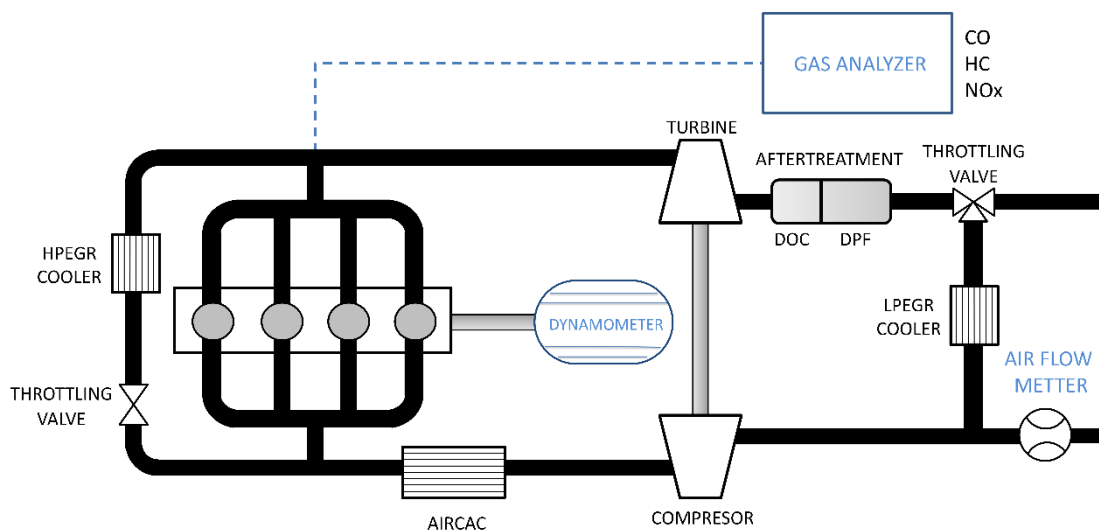


Fig 1. Engine layout.

The tests were carried out in a climatic chamber where the ambient, coolant and fuel temperatures were under control. In Table 1 the main features of the engine are shown. The engine was run under transient state conditions of NEDC and WLTC driving cycles. Once the tests were finished, the engine was put under specific running conditions to regenerate the particulate filter. After that, the test cell was cooled down for eight hours, following the same procedure as [23], to ensure the same initial conditions of all cycles carried out.

Table 1.

Engine specifications.

Cylinder number	In-line 4
Bore x stroke (mm)	80 x 79.5
Displacement (cm ³)	1598
Compression ratio	15.4:1
Valve number	16
Valvetrain	Double cam shaft over head
Fuel delivery system	Common rail. Direct injection.
EGR system	HP and LP cooled EGR
Intake boosting	Turbocharger with VGT
Maximum power (kW/rpm)	96/4000
Maximum torque (Nm/rpm)	320/1750
Torque at maximum power (Nm)	315
Specific power (kW/liter)	60.86

Relevant variables of the test needed for the analysis were recorded: engine speed, torque, intake manifold pressure, turbine inlet pressure, intake manifold temperature, air mass flow rate, fuel consumption and chemical species such as carbon monoxide (CO), hydrocarbons (HC) and nitrogen oxides (NO_x). All measurements were sampled at 10 Hz.

Engine speed was measured through a KISTLER encoder with an uncertainty of 0.02 Crank Angle Degree (CAD). Engine torque was measured by the SCHENK DYNAS3 dynamometer, with an error of 0.1%. The engine speed and torque are the engine target variables needed to perform the driving cycles. Both variables are calculated from the vehicle velocity and the gear ratio defined by the driving cycles and the features of the vehicle. The vehicle model used for the tests was a typical mid-size car from the

European market. The calculation process of the driving cycle target variables is as follows:

The engine speed is calculated from the vehicle speed and gear according to the following expression:

$$n = \frac{u}{\pi \cdot D \cdot Z} \quad [1]$$

Where n is the engine speed, Z is the gearbox ratio between the driven and the drive gear, u is the vehicle speed and D is the diameter of the car wheel.

The engine power demand is calculated from the increase of vehicle kinetic energy, the loss terms and the mechanical efficiency of the gearbox.

$$P = \left(\frac{m(u^2_{t+1} - u^2_t)}{2t} + P_{road} + P_{aerodynamic} \right) \cdot \frac{1}{\eta_m} \quad [2]$$

where P is the crankshaft power, m is the vehicle mass, u is the vehicle speed, t is the time between two points of the driving cycle, P_{road} is the road friction power loss, $P_{aerodynamic}$ is the aerodynamic power loss and η_m is the mechanical efficiency of the gear box. The first term of the sum represents the increase of kinetic energy of the vehicle. In case of no velocity variation, the demand of power is only owing to the frictional losses. Road and aerodynamic friction losses are vehicle speed dependent.

Once the crankshaft power and the engine speed are obtained, the engine torque, N , is calculated as:

$$N = \frac{P}{2 \cdot \pi \cdot n} \quad [3]$$

Temperatures were measured with type K thermocouples of TCA brand, with a measurement error of 2.2 K. Gas pressure was measured with KISTLER pressure sensors with an error of 0.3%. Air mass flow rate was measured by means of a hot wire anemometer of Sensyflow brand, with a measurement error of 0.1%. Fuel consumption along the WLTC cycle was measured with an AVL fuel balance, with a measurement error of 0.12%.

A HORIBA MEXA ONE gas analyser was used to measure the exhaust gas chemical composition upstream the DOC. CO was measured by using Non-Dispersive Infrared (NDIR) absorption, HC was measured by means of the Flame Ionization Detection (FID) technique and NO_x by means of Chemiluminescence Detection (CLD) [34]. The uncertainty of the gas analyser is in the range of 2%.

2.2 Pollutant emissions calculation

Once the chemical pollutants have been measured by the gas analyser, it is necessary to process the data to ensure the right time span and avoid the mismatch between pollutant emissions and the other engine variables such as air and fuel mass flow [24]. The existence of a delay in pollutant analysis is due to two different sources [25]. On one hand, there is an internal delay necessary to analyse the sample that depends on the type of pollutant. On the other hand, the distance between the sample point and the gas analyser forces the existence of a delay defined by the gas velocity and the length of the sample pipes. The gas speed through the sample pipes is produced by the vacuum pressure generated by the gas analyser pump, which remains equal during the whole cycle. Some authors have implemented physical behaviour models [26] while other authors analyse the delay by correlation methods comparing the pollutant measurement with other related variables like engine speed and air mass flow rate [27]. In this study a correlation method is used, based on the convolution between pollutants and air mass flow signals [28]. Convolution expresses the amount of overlap between two functions; it is defined as the integral of the product of two signals when one of these functions is shifted over the other:

$$(p * m)(t) = \int_{-\infty}^{+\infty} p(\tau) \cdot m(t - \varphi) d\tau \cong \sum_{i=0}^{i=n} p_i \cdot m_{i-k} \quad [4]$$

where p and m are the pollutant and air mass flow signals in the time domain (t). φ is the shift variable. The right hand side of the equation is an approximation of the convolution between functions in case they are finite discrete signals. p_i and m_{i-k} are expressed in vector notation, where i is any point of the signal of the n measured

points, k works as shift coefficient. The point where the convolution function is maximum indicates the mismatch delay between signals that must be corrected to synchronize both measurements.

Mass flow rate emissions are calculated using the pollutant concentrations and the air and fuel mass flow rate, according to the equation below. Detailed description of the pollutants emission rates calculation can be found at [29].

$$\dot{m}_{pollutant} = \frac{M_{pollutant}}{M_{air}} \cdot (\dot{m}_{air} + \dot{m}_{fuel}) \cdot [C_{pollutant}]^* \quad [5]$$

Where $M_{pollutant}$ and M_{air} are the molecular weight of pollutants and air respectively \dot{m}_{air} and \dot{m}_{fuel} are the mass flow of fresh air and fuel respectively and $[C_{pollutant}]^*$ is the corrected pollutant concentration. Species concentration measurements such as CO and NO_x are carried out in dry basis, so the concentration is corrected in order to take into account the exhaust gas water vapor content because of the combustion as well as the ambient humidity where the chemical products are being released. Pollutant measurements are corrected according to European Commission Directive 2001/63/EC adapting to technical progress Directive 97/68/EC [30].

2.3 Repeatability and test uncertainty calculation

In addition to the errors of the measurement devices, engine performance and boundary test conditions variability affects the result obtained. Beyond the accuracy of the engine actuators and sensors such as fuel injectors, variable geometry turbine position control and engine speed encoder among others, it is observed a variability when the same test is performed several times. A procedure for anomalous results detection was defined to quantify the natural variability of the process avoiding the presence of exceptions. The outlier detection methodology is divided in two parts. The first part calculates the weighted average of the relative error of test variables. The relative error is weighted by means of the instantaneous variable measurement magnitude. The mathematical

expression is shown below, where the right hand side is the discrete approximation according to Riemann sum.

$$\varepsilon = \frac{\int_0^T \bar{\beta}(t) \cdot \bar{x}(t) dt}{\int_0^T \bar{x}(t) dt} \cong \frac{\sum_{i=0}^{i=n} \bar{\beta}_i \cdot \bar{x}_i}{\sum_{i=0}^{i=n} \bar{x}_i} \quad [6]$$

Where \bar{x} is the instantaneous measured average variable, $\bar{\beta}$ is the instantaneous average relative error of each variable, both obtained from the mean of several repetitions of the same test, and n is the number of test measurement points. $\bar{\beta}$ is calculated as follows:

$$\bar{\beta} = \frac{1}{m} \cdot \sum_{j=0}^{j=m} \alpha_j \quad [7]$$

Where m is the number of test repetitions by case and α is the instantaneous relative error of each test repetition defined as:

$$\alpha_j = \left| \frac{x_j - \bar{x}}{\bar{x}} \right| \quad [8]$$

Where x is the variable under study at the j test repetition.

With the substitution of Eq. 7 and 8, the Eq. 6 can be rewritten in terms of the measured variable as:

$$\varepsilon = \frac{\frac{1}{m} \sum_{i=0}^{i=n} \sum_{j=0}^{j=m} |x_{j,i} - \bar{x}_i|}{\sum_{i=0}^{i=n} \bar{x}_i} \quad [9]$$

The above parameter is a modification of the original definition of the Symmetric Mean Average Percental Error (SMAPE) defined by Flores [31]. The ratio shows how high is the dispersion (expressed as an absolute error) of the whole tests set related to the averaged variable value.

Measured variables, such as pressures, temperatures, fuel mass flow, air mass flow, engine speed, engine torque show a relative error (ε) lower than 5%.

The second part of the outlier detection method focusses on pollutant emissions variability. Because pollutants emissions variation between test repetitions can be high compared to the rest of the test variables [25], an additional analysis based on

cumulative emissions instead of instantaneous measurements is applied. The pollutant mass is calculated at each speed part of the cycles. The pollutants dispersion degree is analysed by means of boxplots where data is divided in quartiles. The threshold to consider a measurement as an outlier occurs when the distance between the pollutant mass and the closest quartile is higher than 1.5 times the interquartile range. In addition, extreme values existence is studied through the comparison of the mean and median of the data set. In case of adding an anomalous test in a sample, the median remains with low variations while the mean is strongly modified. The comparison between median and mean is characterised by the ratio between the absolute difference between the median and mean divided by the median of the data set:

$$SK = \frac{|m-\mu|}{m} \cdot 100 (\%) \quad [10]$$

Where SK is the median-mean skewness coefficient, m and μ are the pollutant median and average of the test, respectively, at each defined time step. This coefficient measures the central tendency of the data set distribution. Considering the experimental variability as a symmetric distribution, the higher this coefficient, the skewed the data set because of the presence of an outlier. The threshold of this coefficient, to consider a measurement as an outlier, is defined as 4%. The threshold value is obtained by Monte Carlo method approach: first, considering the hypothesis of normal error pollutants distribution [32], a normal distribution is created with a mean and a standard deviation obtained from the experimental data set. Then, a large data set is randomly sampled and used to calculate the average of the median-mean skewness coefficient. This procedure is applied at each key point of the driving cycle by pollutant emission. Finally, the highest value obtained of the averaged skewness coefficients is defined as threshold of the SK coefficient.

2.4 Description of NEDC and WLTC

Designed to represent the typical usage of a car in Europe, the NEDC is composed by four repetitions of the Urban Driving Cycle (UDC) and an Extra Urban Driving Cycle

(EUDC), being the total duration 1180 seconds. NEDC has been widely criticized of not being representative of a real driving behaviour where transient conditions get more importance [33] and [14]. Aimed to create a realistic driving cycle, the developing of a worldwide harmonized light duty test cycle (WLTC), that represents the average driving characteristics around the world, was launched by the World Forum for the Harmonization of Vehicle Regulations (WP.29) of the United Nations Economic Commission for Europe (UNECE) through the working party on pollution and energy transport program (GRPE) [15]. WLTC is composed by four phases: low, medium, high and extra high speed, being the total duration 1800 seconds.

Dynamic behaviour of NEDC and WLTC is assessed by the acceleration histogram depicted in Fig 2. Histogram bars are represented in relative frequency, dividing each interval repetition by the total. The relative frequency histogram shows how dynamic is the behaviour of the driving cycles. NEDC performs with low transient conditions during half of the cycle with accelerations bounded between -0.1 and 0.05 m/s^2 . Acceleration distribution is skewed to the left side, pointing that deaccelerations get more important than accelerations, which are critical regarding engine efficiency and pollutant emissions. Regarding the WLTC, the higher dispersion of the histogram is noticeable owing to the more intense dynamic behaviour. Low transient points, delimited in the region of -0.1 to 0.07 m/s^2 , represent just the 30 % of the whole WLTC. Regarding the highest acceleration, the acceleration is limited to 0.83 in the NEDC while in case of the WLTC it reaches the 1.25 m/s^2 .

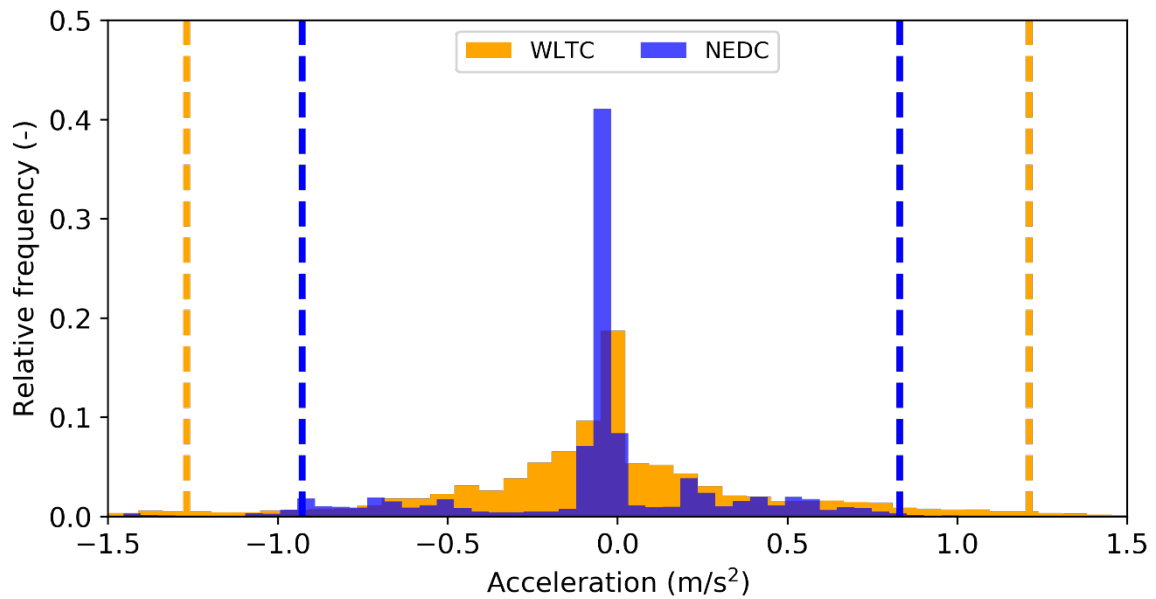


Fig 2. Acceleration normalized histogram of both driving cycles. Dotted lines mark the 95% of values.

The main engine variables such as: torque, engine speed and power are shown in Fig 3 for both driving cycles. All variables have been averaged by driving phase. Regarding the low load part, requested power is similar, 3.25 and 4.5 kW for NEDC and WLTC respectively, being the engine speed higher at the NEDC and therefore the engine torque lower than the WLTC. Concerning higher load parts, EUDC at the NEDC, performs like the high speed part of the WLTC when the engine demand power rises to 11 kW in both cycles, being the torque slightly lower in the NEDC. In case of the WLTC, extra-high speed is performed at the last part of the cycle with a power demand increase to 22.5 kW where the average torque almost reaches the 100 Nm.

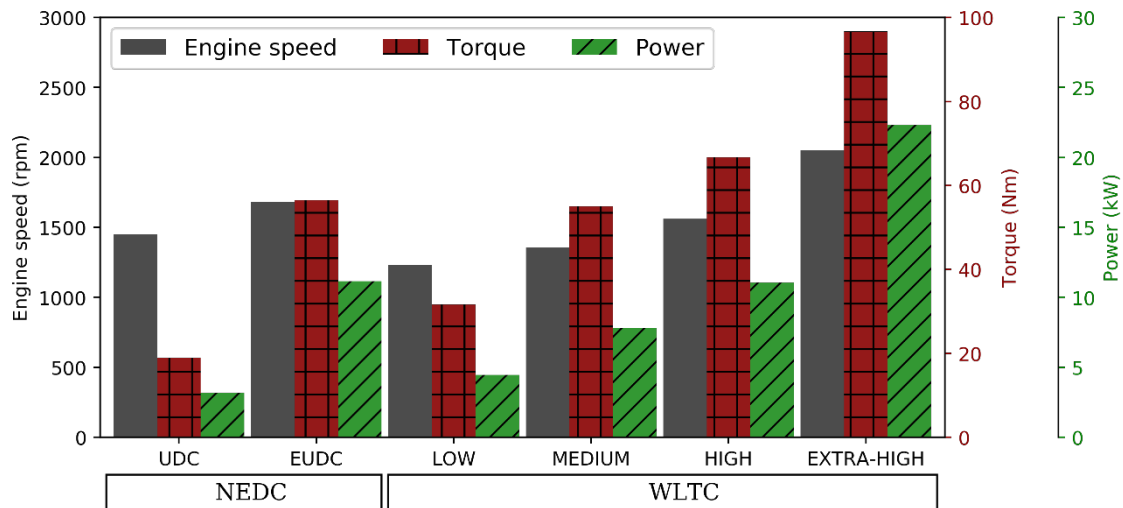


Fig 3. Averaged main engine variables by driving phase in the NEDC and WLTC.

3. Results and discussion

This section describes the effect of ambient temperature on both, NEDC and WLTC, driving cycles by comparing the pollutant emissions and engine efficiency at -7 °C and 20 °C. First, the effect of the ambient temperature on the air management system is addressed. Secondly, the effect of low ambient temperatures on pollutant emissions and brake thermal efficiency is analysed. Finally, a deep analysis on the cold start and first instants of warm up is included remarking the effect of load transients on emissions increase.

3.1 Effect of ambient temperature on the air management system.

The EGR strategy plays a crucial role on the air mass flow performance. When EGR is enabled, air management by the intake manifold pressure is shifted to the air mass flow meter based control. Indeed, under EGR running conditions, air mass flow is not set by the VGT position but by the EGR valves position [36,37,38]. Aimed for NO_x reduction, EGR has become one of the most popular active systems for pollutants reduction in diesel engines. Nevertheless, lowering peak combustion temperature along with oxygen dilution at cold running conditions may drive to combustion instabilities that can increase emission such as HC, CO and particle matter, and eventually result in misfiring events. [39,40].

Fig 4 and Fig 5 show the air mass flow ratio between $-7\text{ }^{\circ}\text{C}$ and $20\text{ }^{\circ}\text{C}$ for NEDC and WLTC respectively. Values have been smoothed by means of a Gaussian convolution filter. Solid gray shadow plots the vehicle speed. In addition to the air mass flow ratio, the EGR valves position are depicted. EGR system performs in similar way in both driving cycles. At $20\text{ }^{\circ}\text{C}$, HP EGR is enabled from the beginning and once the coolant temperature reaches $60\text{ }^{\circ}\text{C}$, around 500 seconds for both cycles, the HP is replaced by the LP EGR. All engine tests were performed under the carmaker calibration. In general carmakers set an engine coolant temperature threshold to enable the exhaust gas recirculation systems. EGR calibration begins with HP EGR and then switches to LP EGR. The reason behind this strategy is to avoid compressor wheel damage owing to water condensation by running LP EGR at low temperature. Engine coolant and intake manifold temperature is generally used by carmakers as EGR control variable. Regarding $-7\text{ }^{\circ}\text{C}$ tests, the HP EGR is enabled when engine coolant temperatures are over $60\text{ }^{\circ}\text{C}$. Concerning the NEDC, EGR is enabled at 1000 seconds, at the last half term of the EUDC, when high engine loads are performed. In case of WLTC as the engine warming up proceeds faster, owing to the higher power demand, the EGR is enabled earlier, at roughly 850 seconds, during the middle engine load.

The effect of EGR on the air mass flow is noticeable looking at the air flow ratio. On one hand, as the EGR remains disabled at $-7\text{ }^{\circ}\text{C}$, the air flow ratio shows great values and performs in unsteady manner. During transients, the ECU control demands lower EGR rates commanding the EGR valve closing. In consequence at these points, the air flow ratio drops. On the other hand, boost control is directed by the intake manifold pressure during cutoff EGR operation points [42]. So, the lower ambient temperature carries higher air density that increases the air mass flow rate. Comparing both: the EGR disabling and the higher air density, the effect of EGR disabling is more meaningful. The air mass flow rise driven by the EGR enabling represents the 85% and 72% of the total increase in the WLTC and NEDC respectively.

During the EGR cut off, air mass flow ratio is bounded between 1.4 – 2.4 and 1.2 – 2.2 in NEDC and WLTC respectively. Once EGR is enabled at -7 °C, air mass flow ratio fluctuations vanish, and amplitude drops to around 1.3 in both driving cycles.

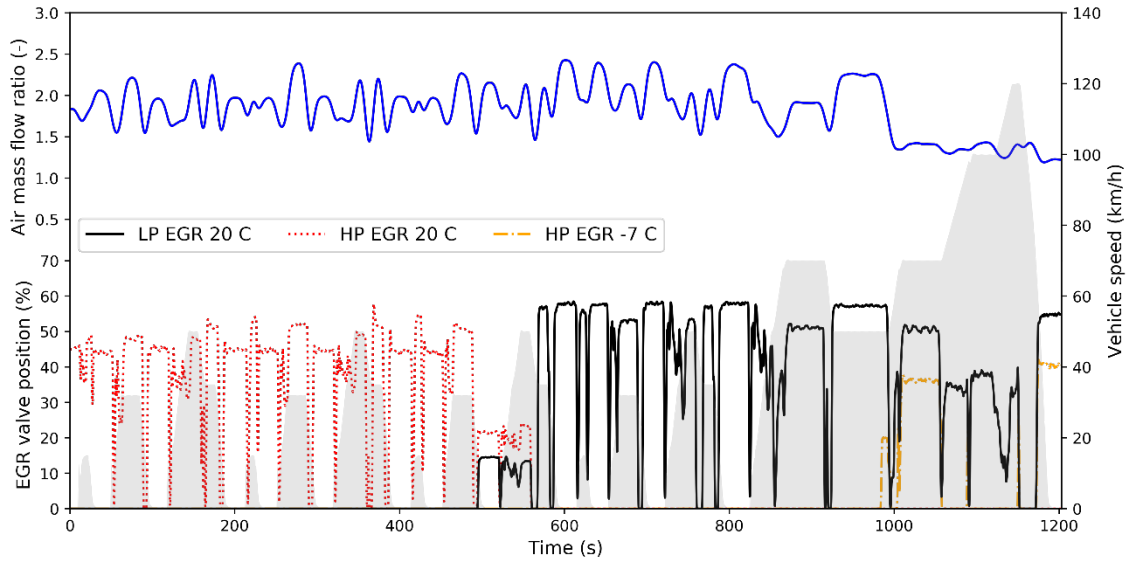


Fig 4. Air mass flow ratio between -7 °C and 20 °C in NEDC and EGR valves positions. Vehicle speed depicted as a surface in grey.

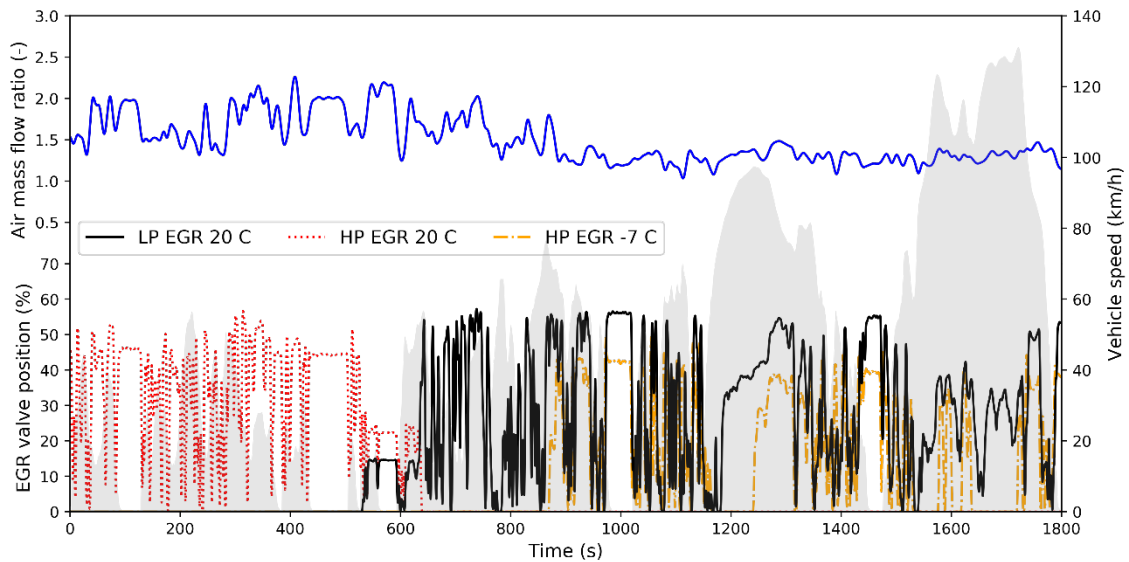


Fig 5. Air mass flow ratio between -7 °C and 20 °C in WLTC and EGR valves positions. Vehicle speed depicted as a surface in grey.

3.2 Pollutants and engine performance by driving phase.

Fig 6 and Fig 7 show the pollutants ratios of HC, NO_x, CO and fuel consumption, by driving phase, between the cold and warm cases for the NEDC and WLTC respectively. Regarding the NEDC, in Fig 6, the evolution of emissions shows similar patterns between HC, CO and fuel consumption. In general terms, these ratios go down as the cycle proceeds.

In the case of hydrocarbons, the emission ratio peak is not placed at the beginning of the cycle but in the second UDC. During cold start, even at 20 °C ambient temperature, significative emissions of HC are released as consequence of the enriched fuel mixture and low temperature combustion [41] that drives to incomplete combustion [12]. In the 20 °C case, the enabling of EGR in the beginning of the engine cold start leads to an increase of HC in detriment. The maximum difference in HC emission is observed during the second UDC. The engine warm up reduces HC at both ambient temperatures, being the HC decrease more significative at 20 °C than at – 7 °C during the first 400 seconds. Beyond this point, HC reduction tends to slow down at 20°C in comparison to the -7 °C case. That's the reason why emissions at -7°C tends to approach the 20 °C case, being the lowest difference on HC emissions at the last driving phase, when high loads are performed, with a ratio of 1.8.

Concerning CO, the ratio decreases monotonically from 3.4 at the beginning to 1.4 at the end of the EUDC. As for the fuel consumption, ratios perform with low variations along the NEDC, being the highest ratio of fuel consumption 1.4 at the beginning and the lowest 1.1 when high loads are performed.

In contrast to carbon based emission, NO_x ratios show a non-monotone evolution with high emissions at – 7° C during the EUDC. As the negative effect of cold start on emissions is greater at low ambient temperatures, NO_x shows higher ratios at the first UDC than at the second and third UDC. According to Zeldovich mechanism [43], NO_x is produced in conditions of high oxygen concentration and temperature. Both variables are lowered by EGR valve opening, driving eventually to NO_x reduction. As was shown

in Fig 4, EGR remains disabled at -7 °C until 1000 seconds. On contrast, EGR is running from the beginning in the 20 °C case. At the last UDC, the increase of NOx ratio is driven by the switch from HP to LP EGR in the 20 °C case. Finally, at the EUDC, NOx emissions get more important because of the higher engine loads. As LP EGR is enabled at 20 °C, high EGR rates and low combustion temperatures can be achieved. In contrast, EGR is not enabled at -7 °C until the 1000 seconds by means of the HP EGR loop whose ability of NOx reduction is lower than LP EGR [44] and [45].

Evaluating the whole NEDC, the effect of lowering the ambient temperature to -7 °C leads to an increase of 270% in HC, 125% in CO and 250% in NOx. Regarding fuel consumption, an increase of 10% is observed.

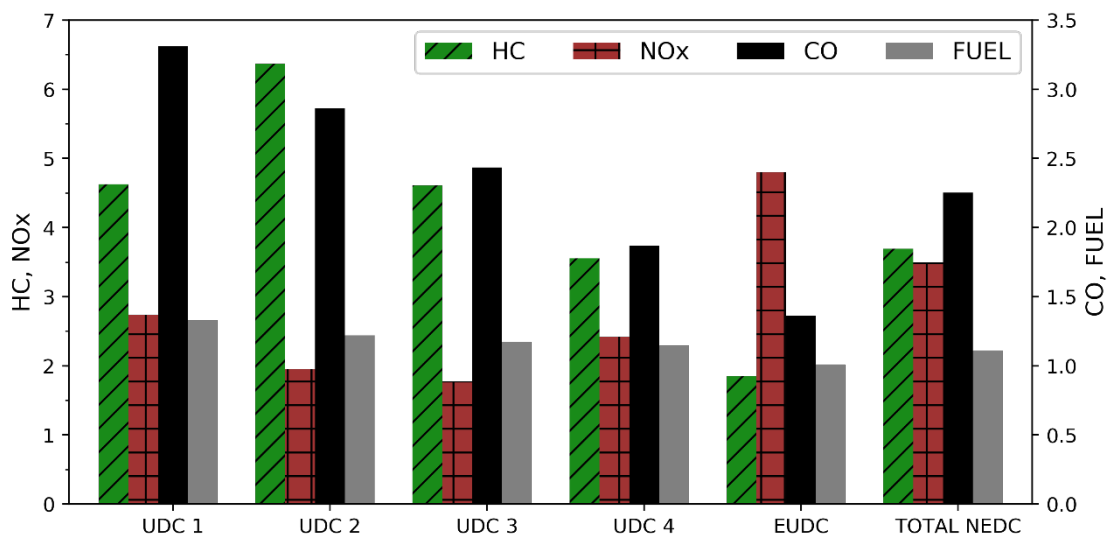


Fig 6. Pollutant and fuel ratio by driving phase in NEDC. HC and NOx on the left axis. CO and fuel consumption on the right axis.

Concerning WLTC, ambient temperature effect on pollutants and thermal engine efficiency is shown in Fig 7. As in the NEDC, HC and NOx emissions drastically increase when engine runs at low ambient temperature.

HC emissions evolve in opposite way than NOx, as engine warm up proceeds, hydrocarbons go down and NOx increases. Encouraged by the higher engine loads, the EGR is enabled earlier in WLTC, at 875 seconds, than in NEDC, at 1000 seconds.

Despite HP EGR is enabled during the WLTC middle speed phase, performed EGR rates are not enough to reduce NO_x emissions as LP EGR does. At the extra-high part, the NO_x at -7 °C rises to 6.2 times the emission at 20 °C.

In the case of CO, emissions perform in a quite different manner. Maximum ratio is bounded to 1.3, at the low speed WLTC phase, and suddenly drops when higher loads are performed, being CO emissions at -7 °C lower than at 20 °C. The minimum ratio is obtained during the medium load term where HP EGR is not enabled until the last part of this driving phase. Once EGR is enabled, a slight deterioration on CO emissions at -7 °C is observed owing to the oxygen concentration dilution [45]. CO and HC pollutants formation share similar dependence with combustion temperature and oxygen concentration. In case of NEDC, both species evolve in the same way, being the engine warm up the main responsible of reduction. However, despite HC emissions are closely linked to CO emissions since they are both caused by low quality combustion, [45] and [46], in WLTC this correlation is not found. Results suggest that CO emissions are more sensitive to oxygen concentration than HC [45]. Under strong load transient conditions air management control becomes crucial to ensure proper air cylinder filling and exhaust gases removing. When required Air to Fuel Ratio (AFR) is not achieved, incomplete combustion occurs and consequently CO emissions increase. When EGR is enabled, air management becomes harder to control and ensure complete combustion. During transients, ECU commands the EGR valve closing, as observed in Fig 5, to fulfil power demands and avoid soot emissions increase [47], [48] and [49]. The effect of transients on CO is more significant at 20 °C than at -7 °C owing to the higher EGR rates performed by the LP than HP EGR, as well as the lower intake temperature of the air-EGR mixture. Evaluating the whole WLTC, the effect of lowering the ambient temperature to -7 °C leads to an increase of 150% in HC, 280% in NO_x and a reduction in CO of 18%. Regarding fuel consumption, an increase of 1% is observed. As variation is lower than

the test repeatability uncertainty threshold of 5%, as explained in Section 2, deterioration of brake thermal engine efficiency cannot be considered.

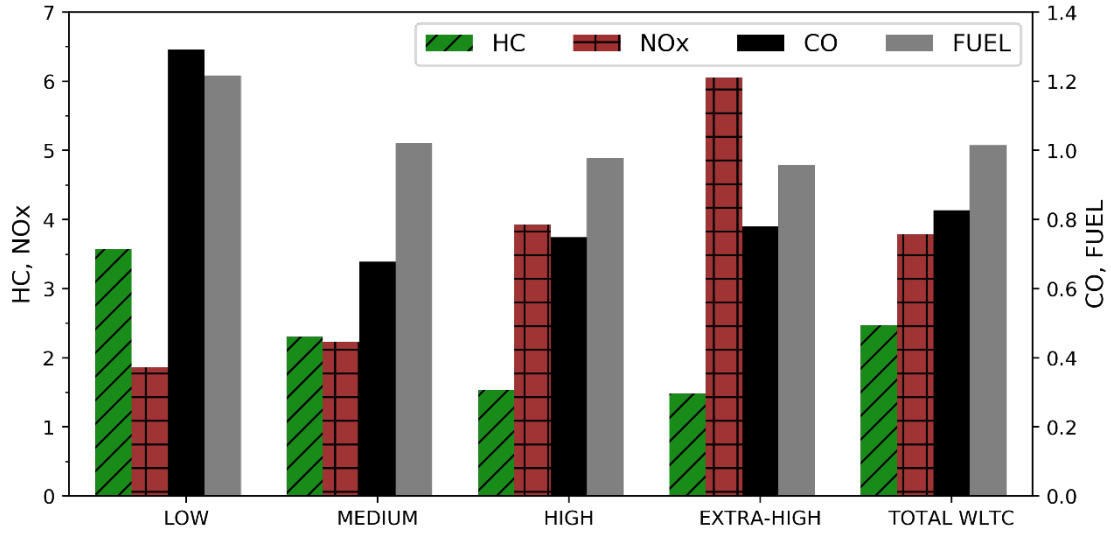


Fig 7. Pollutant and fuel ratio by driving phase in WLTC. HC and NOx on the left axis. CO and fuel on the right axis.

3.3 Pollutants comparison between NEDC and WLTC

In this section cumulated emissions of both driving cycles are shown. As engine loads perform in very different manner between NEDC and WLTC, to compare the evolution of pollutants along the driving cycle the emissions must be rescaled previously. The comparison of pollutants between driving cycles is based on the ratio between the cold and warm cycle. The emissions ratios by cycle are rescaled as follows:

$$R_{x_scaled} = \frac{R_x - \min(R_x)}{\max(R_x) - \min(R_x)} \quad [11]$$

where R_x is the ratio between the cold and warm cycle of each cumulated mass emission.

$$R_x = \frac{\int_0^{ti} \dot{m}_{x_cold}}{\int_0^{ti} \dot{m}_{x_warm}}, \quad ti \in [0, 0.1, 0.2, \dots T] \quad [12]$$

T is the total duration of each cycle, 1200 seconds for NEDC and 1800 seconds for WLTC. In Fig 8, pollutant emissions ratios are depicted for both NEDC and WLTC. HC ratios evolve along the NEDC and WLTC in a very similar way, being the peak of emissions placed at 400 seconds in both cycles. Beyond this point, the HC cumulated

ratio reduces owing to the engine warm up at -7 °C. The fact that both cycles perform with great similarities suggests that HC are more sensitive to the engine warm up than to the EGR strategies. The engine heating up has been analysed by the rejected thermal energy of the in-cylinder energy balance, according to the following expression.

$$RH = \dot{m}_f \cdot LHV + \dot{m}_{air} \cdot c_p \cdot T_{in} - (\dot{m}_{air} + \dot{m}_f) \cdot c_p \cdot T_{exh} - N \cdot 2 \cdot \pi \cdot n \quad [13]$$

where RH is the rejected heat power, \dot{m}_f and \dot{m}_{air} are the fuel and air mass flow rate respectively, T_{in} and T_{exh} are the intake and exhaust manifold temperature, N is the torque, n is the engine speed, LHV is the Low Heating Value of the fuel and c_p is the heat capacity at constant pressure. The above expression is composed by four terms. From the left to the right: the two first terms are the in-cylinder power inputs as the heat released at the combustion and the intake air enthalpy. The two last terms address the output power terms such the exhaust gases enthalpy and the mechanical brake power. The rejected thermal energy comprises the engine mass, coolant and oil heating up as well as the energy released to the surroundings. Cumulated rejected energy and engine coolant temperatures along the cycle are shown in Fig 9 for both NEDC and WLTC at -7 °C. Regarding the rejected energy, both cycles follow the same tendency pointing that the warming up proceeds with the same heating rate in both cycles. This shared warming up behaviour is spotted also by comparing the coolant temperature of both driving cycles.

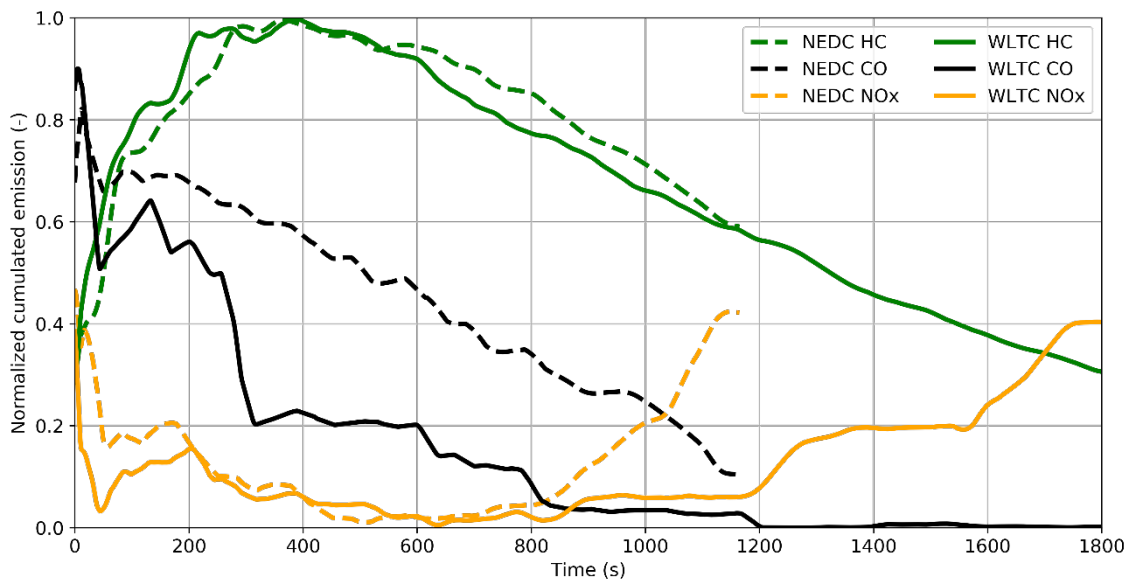


Fig 8. Rescaled cumulated emissions ratio. Dotted lines for NEDC and solid lines for WLTC.

In the same way, NO_x emissions behave in such quite similar manner too. Both cycles show the same peak emission at the beginning. As the cycles proceed, until 800 seconds, both NO_x ratios reduce because of the cold start effect vanishing, the low intake temperature and the low loads performed that downplay the role of EGR on NO_x reduction. Once higher loads are performed, beyond the 800 seconds in NEDC and 1200 in WLTC, HP EGR at -7 °C is not enough to keep the NO_x low and therefore an increase in the NO_x ratio is observed in the last term of both cycles. Unlike HC and NO_x, CO shows quite different patterns. Reductions are stronger in WLTC where CO is even lower at -7 °C than at 20 °C, as already shown in Fig 7. Higher emissions are measured at the beginning of the cold start. But, after 50 seconds significant reductions are observed comparing -7 °C to 20 °C. The EGR control along with the heavy transient conditions makes CO evolution at -7 °C sharper comparing the WLTC to NEDC, where CO ratios evolve like HC does, with a quite constant and similar rate of decreasing. In the case of CO, the air management control, driven by the EGR system, plays the main role on emissions mostly during transient conditions, causing important differences between NEDC and WLTC.

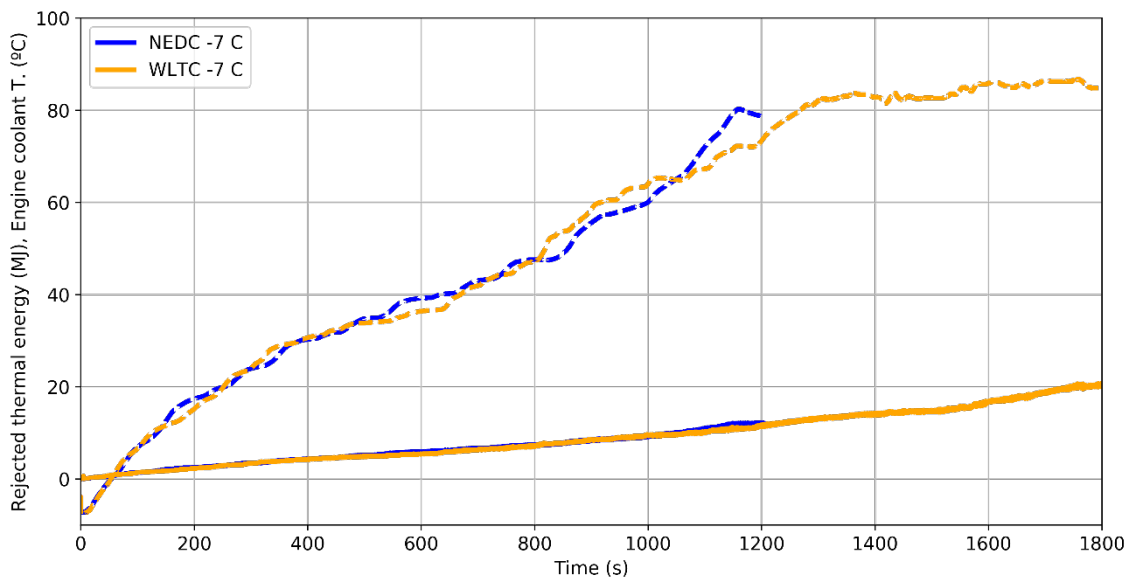


Fig 9. Rejected heat (solid lines) and Engine coolant temperature (dotted lines) of the NEDC and WLTC cycles at -7 °C.

3.4 Instantaneous emissions during engine warm-up

In addition to the analysis by driving phase and cumulated pollutants along the cycles, the instantaneous emission rates are depicted in Fig 10 and Fig 11 for the NEDC and WLTC respectively. Concerning the NEDC, in Fig 10, the first two UDC, first 400 seconds, are shown. High CO and HC peak emissions are observed at the beginning of the cycle at -7 °C. Significant differences are observed between cold and warm cycles at steady state conditions, being remarkable the increase in HC. After the first 50 seconds both pollutants, HC and CO, perform in similar manner: most of pollutants are released during steady state conditions being the effect of transients less significant. In case of NOx, the emission rate evolves in opposite way being the effect of transients the main cause of emission. Despite emissions rate is a bit higher at 20 °C in some points of vehicle acceleration, like at 50 ,120 and 215 seconds among others, the effect of transients is greater at -7 °C than at 20 °C.

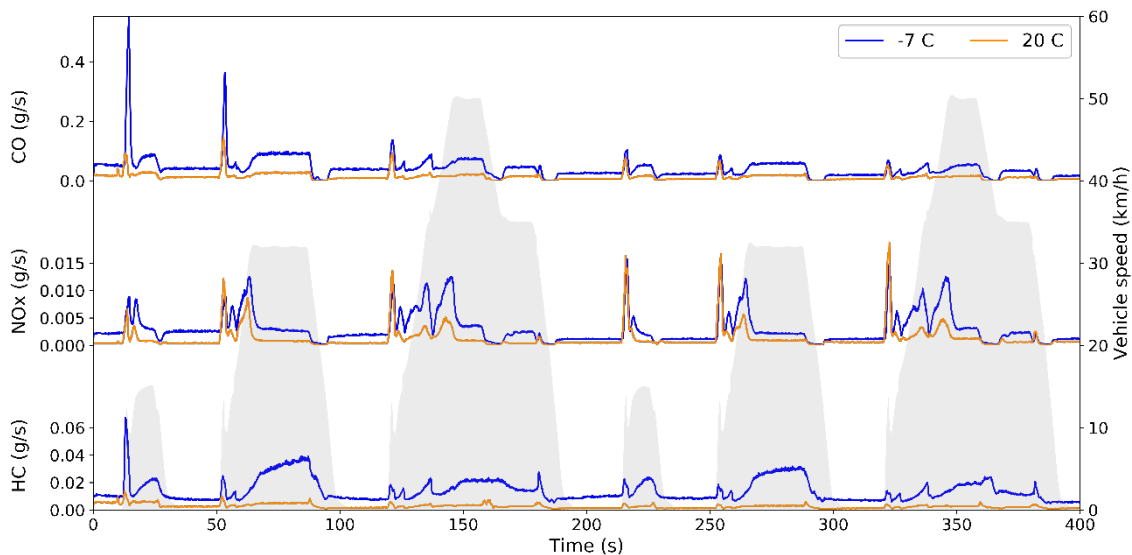


Fig 10. Instantaneous emission rates for HC, CO and NOx in NEDC. Vehicle speed depicted as a surface in gray.

WLTC emission flow rates are depicted in Fig 11, for the first (low speed) part of the cycle, first 600 seconds. High HC peak is observed at the -7 °C cold start. Unlike was seen in the NEDC, HC and CO emissions don't evolve with similar patterns in the WLTC. Hydrocarbons show similar dependence with load regardless the transient engine loads of the cycle. But, in the case of CO, transient conditions play the main role as emission source, being the CO emissions during transients up to 140 times the rates produced during steady operations. A zoom of the CO flow rates, between the 50 and 120 seconds, is included in Fig 11. During low transient points, CO emissions are higher at -7 °C than at 20 °C as in the NEDC. However, during strong transients, e.g. at 250 seconds, CO flow rates are considerably higher at 20 °C, being up to twice the emission rate of -7 °C. Transients make the accumulated CO emitted mass be higher at 20 °C than at -7 °C. In the case of NOx, emission rates evolve similar to the NEDC. Peak emissions are a bit higher at 20 °C under strong transients, but this tendency flips in steady running conditions where NOx is much higher at -7 °C and eventually makes the cumulate mass at -7 °C higher than at 20 °C.

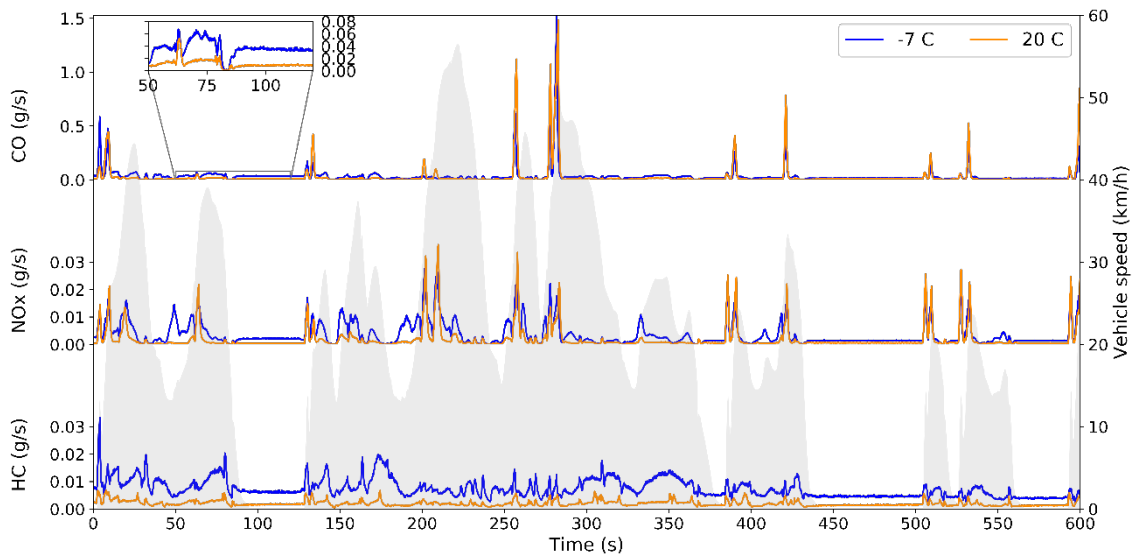


Fig 11. Instantaneous emission rates for HC, CO and NOx in WLTC. Vehicle speed depicted as a surface in gray.

4. Conclusions

The effect of low ambient temperature on pollutant emissions is analysed. WLTC and NEDC were carried out at two levels of ambient temperature: -7 °C and 20 °C. Pollutant analysis was focused on carbon monoxide, unburned hydrocarbons and nitrogen oxides. Thermal efficiency was evaluated by means of the fuel consumption. In general terms, emissions are increased and thermal efficiency is deteriorated when the engine runs at low ambient temperatures.

The negative effect of low ambient temperatures is more significant in the NEDC than in the WLTC. The whole emissions and fuel consumption ratio, between the cold and warm test, of both driving cycles is depicted in Fig 12 . Hydrocarbons emissions are 3.7 times higher in the NEDC while in the WLTC are bounded to 2.5. Regarding NO_x, similar tendencies are observed being the emissions around 3.5 and 3.8 higher at low ambient temperatures for the NEDC and WLTC respectively. Concerning CO, opposite tendencies between both cycles are observed with the increase to 2.25 in the NEDC and the reduction to 0.82 in the WLTC. In the case of fuel consumption, the effect of low temperatures is remarkable in the NEDC with an increase around 10%. On the other hand, no fuel penalty is spotted in the WLTC.

Fig 12 HC, CO, NO_x and fuel ratios in NEDC and WLTC for the whole driving cycle.

The analysis by pollutant shows a significant link between NEDC and WLTC regarding HC emissions. The engine warming up and load play the main role as emission source. Concerning NO_x and CO, the transient conditions of the cycles are the main cause of

pollutant emissions. At strong transient loads, where high demands of power must be met, the air management control is enforced to command the EGR valves closing producing an increase on NO_x emissions. Despite the EGR valve closing, required oxygen concentration is not fulfilled and, consequently, emissions of CO rise. This effect is more noticeable in the WLTC where the role of air management control is critical. As EGR is performed with lower rates and higher temperatures at -7 °C, the effect of transients on the air management gets less important and the amount of CO is lower than at 20 °C.

5. Acknowledgments

The authors of this paper wish to thank Juan Antonio López Cascant for his invaluable work during the laboratory setup and the experimental campaign. Authors also want to acknowledge the “Apoyo para la investigación y Desarrollo (PAID)”, grant for doctoral studies (FPI S1 2015 2512), of Universitat Politècnica de València.

References

1. Reşitoğlu, İ.A., Altinişik, K. & Keskin, A. The pollutant emissions from diesel-engine vehicles and exhaust aftertreatment systems, *Clean Techn Environ Policy* (2015) 17: 15.
2. Qinming Tan, Yihuai Hu, A study on the combustion and emission performance of diesel engines under different proportions of O₂ & N₂ & CO₂, *Applied Thermal Engineering*, Volume 108, 5 September 2016, Pages 508-515.
3. Serrano, J. R., Arnau, F. J., Martin, J., Hernandez, M., & Lombard, B. (2015). Analysis of Engine Walls Thermal Insulation: Performance and Emissions (No. 2015-01-1660). SAE Technical Paper.
4. EPA regulation. 40 CFR Ch. I (7–1–12 Edition). 86.1828–01. Page 452.
5. Commission Regulation (EC) No 692/2008 of 18 July 2008 implementing and amending Regulation (EC) No 715/2007 of the European Parliament and of the Council on type-approval of motor vehicles with respect to emissions from light passenger and commercial vehicles (Euro 5 and Euro 6) and on access to vehicle repair and maintenance information
6. Torregrosa, A. J., Olmeda, P., Martin, J., & Degraeuwe, B. (2006). Experiments on the influence of inlet charge and coolant temperature on performance and emissions of a DI Diesel engine. *Experimental Thermal and Fluid Science*, 30(7), 633-641.
7. Torregrosa, A. J., Broatch, A., Olmeda, P., & Romero, C. (2008). Assessment of the influence of different cooling system configurations on engine warm-up, emissions and fuel consumption. *International Journal of Automotive Technology*, 9(4), 447-458.

8. Weilenmann, M., Favez, J. Y., & Alvarez, R. (2009). Cold-start emissions of modern passenger cars at different low ambient temperatures and their evolution over vehicle legislation categories. *Atmospheric environment*, 43(15), 2419-2429.
9. Li, Q., Shayler, P. J., McGhee, M., & La Rocca, A. (2017). The initiation and development of combustion under cold idling conditions using a glow plug in diesel engines. *International Journal of Engine Research*, 18(3), 240-255.
10. Tautzia, X., Maiboom, A., Karaky, H., & Chesse, P. (2018). Experimental analysis of the influence of coolant and oil temperature on combustion and emissions in an automotive diesel engine. *International Journal of Engine Research*.
11. Ludykar, D., Westerholm, R., & Almen, J. (1999). Cold start emissions at +22, -7 and -20 °C ambient temperatures from a three-way catalyst (TWC) car: regulated and unregulated exhaust components. *Science of the Total Environment*, 235(1), 65-69.
12. Weilenmann, M., Soltic, P., Saxer, C., Forss, A. M., & Heeb, N. (2005). Regulated and nonregulated diesel and gasoline cold start emissions at different temperatures. *Atmospheric environment*, 39(13), 2433-2444.
13. Dardiotis, C., Martini, G., Marotta, A., & Manfredi, U. (2013). Low-temperature cold-start gaseous emissions of late technology passenger cars. *Applied energy*, 111, 468-478.
14. Pavlovic, J., Marotta, A., & Ciuffo, B. (2016). CO₂ emissions and energy demands of vehicles tested under the NEDC and the new WLTP type approval test procedures. *Applied Energy*, 177, 661-670.
15. Tsokolis, D., Tsiakmakis, S., Dimaratos, A., Fontaras, G., Pistikopoulos, P., Ciuffo, B., & Samaras, Z. (2016). Fuel consumption and CO₂ emissions of

- passenger cars over the New Worldwide Harmonized Test Protocol. *Applied Energy*, 179, 1152-1165.
16. Giakoumis, E. G., & Zachiotis, A. T. (2017). Investigation of a Diesel-Engined Vehicle's Performance and Emissions during the WLTC Driving Cycle—Comparison with the NEDC. *Energies*, 10(2), 240.
 17. Myung, C. L., Jang, W., Kwon, S., Ko, J., Jin, D., & Park, S. (2017). Evaluation of the real-time de-NOx performance characteristics of a LNT-equipped Euro-6 diesel passenger car with various vehicle emissions certification cycles. *Energy*, (132), 356-369.
 18. Marotta, A., Pavlovic, J., Ciuffo, B., Serra, S., & Fontaras, G. (2015). Gaseous emissions from light-duty vehicles: moving from NEDC to the new WLTP test procedure. *Environmental science & technology*, 49(14), 8315-8322.
 19. Luján, J. M., Climent, H., García-Cuevas, L. M., & Moratal, A. (2018). Pollutant emissions and diesel oxidation catalyst performance at low ambient temperatures in transient load conditions. *Applied Thermal Engineering*, 129, 1527-1537.
 20. Ko, J., Jin, D., Jang, W., Myung, C. L., Kwon, S., & Park, S. (2017). Comparative investigation of NOx emission characteristics from a Euro 6-compliant diesel passenger car over the NEDC and WLTC at various ambient temperatures. *Applied Energy*, 187, 652-662.
 21. Armas, O., García-Contreras, R., Ramos, Á., & López, A. F. (2014). Impact of animal fat biodiesel, GTL, and HVO fuels on combustion, performance, and pollutant emissions of a light-duty diesel vehicle tested under the NEDC. *Journal of Energy Engineering*, 141(2), C4014009.
 22. E. Zervas, Parametric study of the main parameters influencing the catalytic efficiency of a diesel oxidation catalyst: parameters influencing the efficiency

- of a diesel catalyst, *Int. J Automot. Technol.* 9 (2008) 641.
23. Armas, O., García-Contreras, R., & Ramos, A. (2016). On-line thermodynamic diagnosis of diesel combustion process with paraffinic fuels in a vehicle tested under NEDC. *Journal of cleaner production*, 138, 94-102.
 24. Luján, J. M., Climent, H., Dolz, V., Moratal, A., Borges-Alejo, J., & Soukeur, Z. (2016). Potential of exhaust heat recovery for intake charge heating in a diesel engine transient operation at cold conditions. *Applied Thermal Engineering*, 105, 501-508.
 25. Robinson, K., Ye, S., Yap, Y., & Kolaczowski, S. T. (2013). Application of a methodology to assess the performance of a full-scale diesel oxidation catalyst during cold and hot start NEDC drive cycles. *Chemical Engineering Research and Design*, 91(7), 1292-1306.
 26. Messer, J. T., Clark, N. N., & Lyons, D. W. (1995). Measurement delays and modal analysis for a heavy duty transportable emissions testing laboratory (No. 950218). SAE Technical Paper.
 27. Konstantas, G., & Stamatelos, A. (2004). Quality assurance of exhaust emissions test data. *Proceedings of the Institution of Mechanical Engineers, Part D: Journal of Automobile Engineering*, 218(8), 901-914.
 28. Pakko, J. D. (2009). Reconstruction of Time-Resolved Vehicle Emissions Measurements by Deconvolution. *SAE International Journal of Fuels and Lubricants*, 2(2009-01-1513), 697-707.
 29. Armas, O., Garcia-Contreras, R., & Ramos, A. (2013). Emissions of light duty vehicle tested under urban and extraurban real-world driving conditions with diesel, animal fat biodiesel and GTL fuels (No. 2013-24-0176). SAE Technical Paper.

30. Directive 97/68/EC of the European Parliament and of the Council of 16 December 1997 on the approximation of the laws of the Member States relating to measures against the emission of gaseous and particulate pollutants from internal combustion engines to be installed in non-road mobile machinery.<http://eur-lex.europa.eu/legalcontent/EN/TXT/?uri=CELEX:31997L0068>.
31. Flores, B. E. (1986). A pragmatic view of accuracy measurement in forecasting. *Omega*, 14(2), 93-98.
32. Kandylas, I. P., Stamatelos, A. M., & Dimitriadis, S. G. (1999). Statistical uncertainty in automotive emissions testing. *Proceedings of the Institution of Mechanical Engineers, Part D: Journal of Automobile Engineering*, 213(5), 491-502.
33. Sileghem, L., Bosteels, D., May, J., Favre, C., & Verhelst, S. (2014). Analysis of vehicle emission measurements on the new WLTC, the NEDC and the CADC. *Transportation Research Part D: Transport and Environment*, 32, 70-85.
34. Adachi, M. and Nakamura, H (2014). *Engine Emissions Measurement Handbook: HORIBA Automotive Test Systems*. SAE International. ISBN. 9780768080124.
35. Bielaczyc, P., Szczotka, A., & Woodburn, J. (2011). The effect of a low ambient temperature on the cold-start emissions and fuel consumption of passenger cars. *Proceedings of the Institution of Mechanical Engineers, Part D: Journal of Automobile Engineering*, 225(9), 1253-1264.
36. Stefanopoulou, A. G., Kolmanovsky, I., & Freudenberg, J. S. (2000). Control of variable geometry turbocharged diesel engines for reduced emissions. *IEEE transactions on control systems technology*, 8(4), 733-745.

37. Ammann, M., Fekete, N. P., Guzzella, L., & Glattfelder, A. H. (2003). Model-based control of the VGT and EGR in a turbocharged common-rail Diesel engine: theory and passenger car implementation (No. 2003-01-0357). SAE Technical Paper.
38. Guzzella, L., & Amstutz, A. (1998). Control of diesel engines. *IEEE Control Systems*, 18(5), 53-71.
39. Peng, H., Cui, Y., Shi, L., & Deng, K. (2008). Effects of exhaust gas recirculation (EGR) on combustion and emissions during cold start of direct injection (DI) diesel engine. *Energy*, 33(3), 471-479.
40. Ramadhas, A. S., & Xu, H. (2016). Influence of Coolant Temperature on Cold Start Performance of Diesel Passenger Car in Cold Environment (No. 2016-28-0142). SAE Technical Paper.
41. Weilenmann, M., Soltic, P., Saxer, C., Forss, A. M., & Heeb, N. (2005). Regulated and nonregulated diesel and gasoline cold start emissions at different temperatures. *Atmospheric environment*, 39(13), 2433-2441.
42. Ammann, M., Fekete, N. P., Guzzella, L., & Glattfelder, A. H. (2003). Model-based control of the VGT and EGR in a turbocharged common-rail Diesel engine: theory and passenger car implementation (No. 2003-01-0357). SAE Technical Paper.
43. Zeldovich YB. (1946). The oxidation of nitrogen in combustion explosions. *Acta Pysichochemica USSR*, Vol. 21, pp. 577-628.
44. Heuwetter, D., Glewen, W., Meyer, C., Foster, D. E., Andrie, M., & Krieger, R. (2011). Effects of low pressure EGR on transient air system performance and emissions for low temperature diesel combustion (No. 2011-24-0062). SAE Technical Paper.

45. Bermúdez, V., Lujan, J. M., Pla, B., & Linares, W. G. (2011). Effects of low pressure exhaust gas recirculation on regulated and unregulated gaseous emissions during NEDC in a light-duty diesel engine. *Energy*, 36(9), 5655-5665.
46. Nitu, B., Singh, I., Zhong, L., Badreshany, K., Henein, N. A., & Bryzik, W. (2002). Effect of EGR on autoignition, combustion, regulated emissions and aldehydes in DI diesel engines (No. 2002-01-1153). SAE Technical Paper.
47. Schubiger, R., Bertola, A., & Boulouchos, K. (2001). Influence of EGR on combustion and exhaust emissions of heavy duty DI-diesel engines equipped with common-rail injection systems (No. 2001-01-3497). SAE Technical Paper.
48. Wang, S., Zhu, X., Somers, L. M. T., & de Goey, L. P. H. (2017). Effects of exhaust gas recirculation at various loads on diesel engine performance and exhaust particle size distribution using four blends with a research octane number of 70 and diesel. *Energy Conversion and Management*.
49. Li, X., Xu, Z., Guan, C., & Huang, Z. (2014). Impact of exhaust gas recirculation (EGR) on soot reactivity from a diesel engine operating at high load. *Applied Thermal Engineering*, 68(1), 100-106.